

CONF. 750908--2
EXPERIMENTAL AND ANALYTICAL RESULTS FOR A PRESTRESSED CONCRETE
REACTOR VESSEL MODEL UNDER SIMULATED HTR OPERATING CONDITIONS*

J. P. Callahan J. M. Corum
G. D. Whitman

Oak Ridge National Laboratory
Oak Ridge, Tennessee 37830

NOTICE

This report was prepared as an account of work sponsored by the United States Government. Neither the United States nor the United States Energy Research and Development Administration, nor any of their employees, nor any of their contractors, subcontractors, or their employees, makes any warranty, express or implied, or assumes any legal liability or responsibility for the accuracy, completeness or usefulness of any information, apparatus, product or process disclosed, or represents that its use would not infringe privately owned rights.

MASTER

1. Introduction

Prestressed Concrete Reactor Vessels (PCRVs) are unique when compared with more traditional concrete structures because of the elevated operating temperatures employed and the thorough understanding of structural behavior required to assure safety. In the United States a comprehensive program for developing and improving PCRVs has been undertaken by the Oak Ridge National Laboratory. As part of this effort, analytical methods and concrete materials characterization data have been developed. By incorporating the resulting data into an appropriate analysis method, predictions can be made of the time-dependent behavior of PCRVs subjected to anticipated nuclear reactor operating conditions. The thermal cylinder experiment described herein was designed to provide the information required to assess the capability of analytical methods to predict the structural behavior of operating PCRVs.

2. Thermal Cylinder Design

The thermal cylinder is approximately a 1/6-scale model of the middle section of the cylindrical portion of a single-cavity PCRV subjected to the simulated in-service operating conditions indicated in Fig. 1. The test structure, shown isometrically in Fig. 2, is a thick-walled cylinder having a height of 1.22 m, a thickness of 0.3 m and an outer diameter of 2.06 m. To prevent net moisture loss, the outer and inner liners are continuously welded to the sheet metal seal shown in Fig. 2 and the top surface is sealed using a combination of sheet copper and epoxy. The ends of the model are insulated thermally to prevent heat flow in the axial direction. A calrod-type of electrical resistance heater is wrapped around the inner heat exchanger at the lower third point in order to induce the hot-spot heating condition (not shown in Fig. 2). The model is post-tensioned in both the axial and circumferential directions and the inner cavity of the cylinder contains a concrete core which provides inner support for the relatively thin pressuring annulus as shown in Fig. 2.

3. Instrumentation

The model was instrumented in four quadrant planes, designated by A, B, C, and D, using a total of 155 gages to provide both an evaluation of instrument performance under simulated PCRV design and off-design operating conditions, and experimental data on structural behavior. The instrumentation shown in Fig. 3 for typical locations consists of various types of embedment gages cast into the concrete and conventional electrical resistance strain gages attached to the liner and prestressing tendons. The percent survival of each gage type is shown in Table 1; however, these figures do not reflect gage accuracy or reliability which will be discussed in conjunction with the comparisons of analytical and experimental results.

4. Loading Conditions

The model temperature and loading histories are summarized in Fig. 4. The temperatures shown are for the inner surface while the outer surface was maintained at 75°F (23.9°C) throughout the experiment.

The initial model pressurization period was designed to simulate normal PCRV operating conditions. During the second pressurization period a narrow circumferential band on the inner surface was heated as shown in Fig. 4 to simulate an off-design hot-spot condition produced by an assumed failure of the PCRV thermal barrier. The test structure is described in more detail in Ref. [1] and the model assembly, instrumentation, test history and findings in Refs. [2], [3], and [4].

5. Analytical Results

A time-dependent creep analysis of the thermal cylinder was conducted using the SAFE-CRACK two-dimensional finite-element computer program [5] together with the appropriate materials properties data obtained as part of the overall research program. The analysis employed 47 time steps covering 585 days from completion of prestressing.

The analytical model is an axisymmetric thick-walled cylinder having the dimensions and geometry of the test model. A total of 567 elements are used consisting of triangular ring elements representing the concrete, and membrane shell elements representing the liner or heat exchanger. The circumferential prestressing is represented by uniform pressure applied to the outer barrel section and the axial prestressing tendons are treated as uniaxial tension elements. Once the specified maximum principal strain failure criterion is exceeded,

the affected concrete element is allowed to crack and new stiffness and load matrices are computed in the analysis. The resulting equilibrium equations are then solved for the new displacements.

Comparisons of analytical and experimental results for the type ER circumferentially oriented single-filament concrete embedment gage located immediately adjacent to the hot-spot heater are shown as an example in Fig. 5. Of the various embedment gages employed in the model the type ER precast single-filament resistance type produced the most consistent and meaningful data. In Fig. 5 as was the case in virtually all of the comparisons, the prestressing and pressurization strains were overestimated and those resulting from heat-up were underestimated by the analysis. Although the observed erratic behavior of the strain gages during hot-spot heating can be attributed in part to failures of axial tendons, the equally erratic behavior of the analysis during this period remains to be explained. In general with the exception of a few calculated data points, the experimental and analytical results follow the same trends during the hot-spot experiment.

6. Instrument Performance

The same general trends discussed above were also recorded by the type A vibrating-wire strain gages as shown in Fig. 6 for the average results of the circumferential gages at the innermost position. Since vibrating-wire gages generally function satisfactorily at temperatures below 150°F (65.5°C), failure of this particular set of gages during the hot-spot heating was not unexpected. Although three of the type B vibrating-wire gages continued to function during the entire experiment, the readings were somewhat inconsistent owing to problems with readout instrumentation. When functioning correctly, these gages were in reasonable agreement with the corresponding type A and single-filament resistance gages.

Although the single type C vibrating-wire gage failed to function satisfactorily, this particular hermetically-sealed gage appears in principle to be of superior construction. The manufacturer recommends that these gages be precast in concrete elements to ensure satisfactory performance, which was not done in this study except for the relatively fragile single-filament resistance gages.

The type K wound-wire resistance embedment strain gages failed to function satisfactorily although only one became inoperable during the experiment. Since representative gages of the same type did perform satisfactorily during supplemental short-term loading tests, the unsatisfactory performance of these gages in the thermal cylinder test has been attributed to the absence of bonding between the gage and the concrete. This particular fault should be easily correctable by minor modification of the gage housing. The type T titanium resistance and type PSC pressure diaphragm stress cells employed in the study were experimental types (see Ref. [3] for details) that were found to function satisfactorily during short-term loadings, but behaved inconsistently over extended time periods. Although further development is needed to ensure their reliability and long-term stability, both types of stress cells offer considerable promise.

The same general trends shown for the embedment strain gages also applied to the axial and circumferential weldable strain gages attached to the inner liner. Although the previously noted sharp fluctuations in strain readings were not seen during hot-spot heating, the greatest disagreement between calculated and experimental results for these gages occurred during this period.

7. Prestressing Tendon Performance

Selected individual strands of 12 axial and 8 circumferential prestressing tendons were instrumented with type CG conventional foil resistance strain gages. Also, type TR compression load cells were attached in series with the axial tendons. The load vs time plots of the four tendons adjacent to the C gage quadrant plane are shown in Fig. 7. Load transducers CTR-1 and CTR-3 which were coupled to inner row tendons as shown in the insert figure measured periodic step load drops during the experiment. Recent post mortem studies indicate that these load changes were probably produced by progressive corrosion failure of inner row tendons. The only tendons exhibiting indications of failure during both normal operation and hot-spot heating were the inner axial row. The findings of subsequent chemical and laboratory corrosion tests tend to indicate that the observed tendon corrosion was caused by the presence of moisture and organic impurities in the inadequately sealed tendon ducts, although the actual corrosion mechanism remains to be identified. It should be pointed out that

although the ducts were not hermetically sealed the tendons were coated with a commercial rust preventative and the ducts were filled with a wax which has been used extensively for this purpose. The only other observed change in structural performance was a substantial reduction in strength of concrete within an 8 cm radius of the hot-spot heating element. In addition readings made using a neutron and gamma-ray backscattering moisture probe showed little if any migration of moisture in the concrete cross section.

8. Conclusions

It was concluded that the SAFE-CRACK analysis was reasonably capable of predicting time-dependent behavior in a vessel subjected to normal operating conditions; however, it was unable to accurately predict behavior during off-design hot-spot conditions. The observed tendon corrosion was probably caused by the presence of moisture and organic impurities in the inadequately sealed tendon ducts. Further studies are presently under way to both identify the tendon corrosion mechanism and the reasons for the observed disagreement between analytical and experimental results. Destructive examination indicated that the model maintained its basic structural integrity during localized hot-spot heating.

References

- [1] WHITMAN, G. D., CALLAHAN, J. P., and CORUM, J. M., "An Investigation of the Time-Dependent Behavior of Prestressed Concrete Pressure Vessels," Concrete for Nuclear Reactors, vol. 3, Special Technical Publication SP-34, American Concrete Institute, pp. 823-846 (1972).
- [2] CALLAHAN, J. P., CORUM, J. M., and RICHARDSON, M., "PCRV Thermal Cylinder Test," GCR-TU Programs Annu. Progr. Rep. Sept. 30, 1971, ORNL-4760, pp. 79-91.
- [3] CALLAHAN, J. P., VALACHOVIC, R. S., and ROBINSON, G. C., "PCRV Thermal Cylinder Test," GCR Program Annu. Progr. Rep. Dec. 31, 1972, ORNL-4911, pp. 181-209.
- [4] CALLAHAN, J. P., and ROBINSON, G. C., "PCRV Thermal Cylinder Test," GCR Program Annu. Progr. Rep. (to be published).
- [5] RASHID, Y. R., Nonlinear Quasi-Static Analyses of Two-Dimensional Concrete Structures, GA-9994 (Mar. 23, 1970).

Table 1. Thermal Cylinder Test Gage Survival

Gage type	Letter designation	Total number	Number failed	Percent survival
Embedment gages				
Single filament resistance	(EB)	47	18	61.7
Vibrating wire				
Type A	(D)	27	21	22.2
Type B	(P)	9	3	33.3
Type C	(GA)	1	1	0
Wound wire resistance	(K)	6	1	83.3
Stress cells				
Titanium resistance	(T)	8	3	62.5
Pressure diaphragm	(PSC)	6	6	0
Strain gages				
Weldable (liner)		19	6	68.4
Axial tendons	(CP)	12	3	75.0
Circumferential tendons	(CG)	8	0	100.0
Load cells				
Axial tendons	(TR)	12	1	91.7
Total		155	63	59.4

List of Figures

Fig. 1. Relationship of thermal cylinder test specimen to prestressed concrete react. vessel. (1 psi = 6,895 Pa, $^{\circ}\text{F} = 9/5 ^{\circ}\text{C} + 32$)

Fig. 2. Isometric view of thermal-cylinder test structure. (1 psi = 6,895 Pa, 1 ft = .305 m, 1 lb = .454 kg)

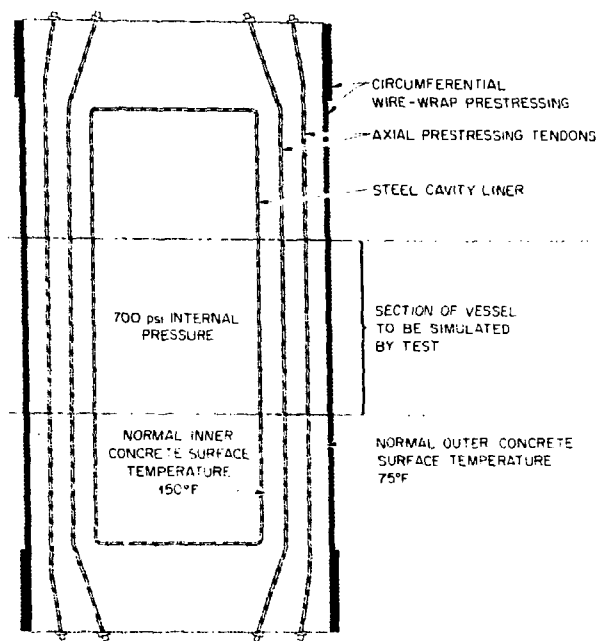
Fig. 3. Typical locations of each embedment gage type in model cross section. (Quadrant planes not shown contain the same types of gages)

Fig. 4. Temperature and loading history of the thermal cylinder model. (1 psi = 6,895 Pa, $^{\circ}\text{F} = 9/5 ^{\circ}\text{C} + 32$)

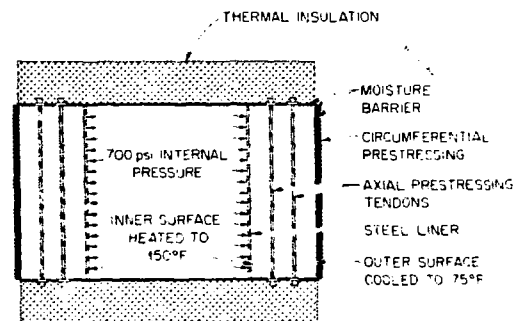
Fig. 5. Theoretical vs experimental strains for type EB circumferential single-filament embedment gage adjacent to hot-spot heaters.

Fig. 6. Theoretical vs experimental strains for average of three circumferential type vibrating-wire embedment gages in position closest to inner liner.

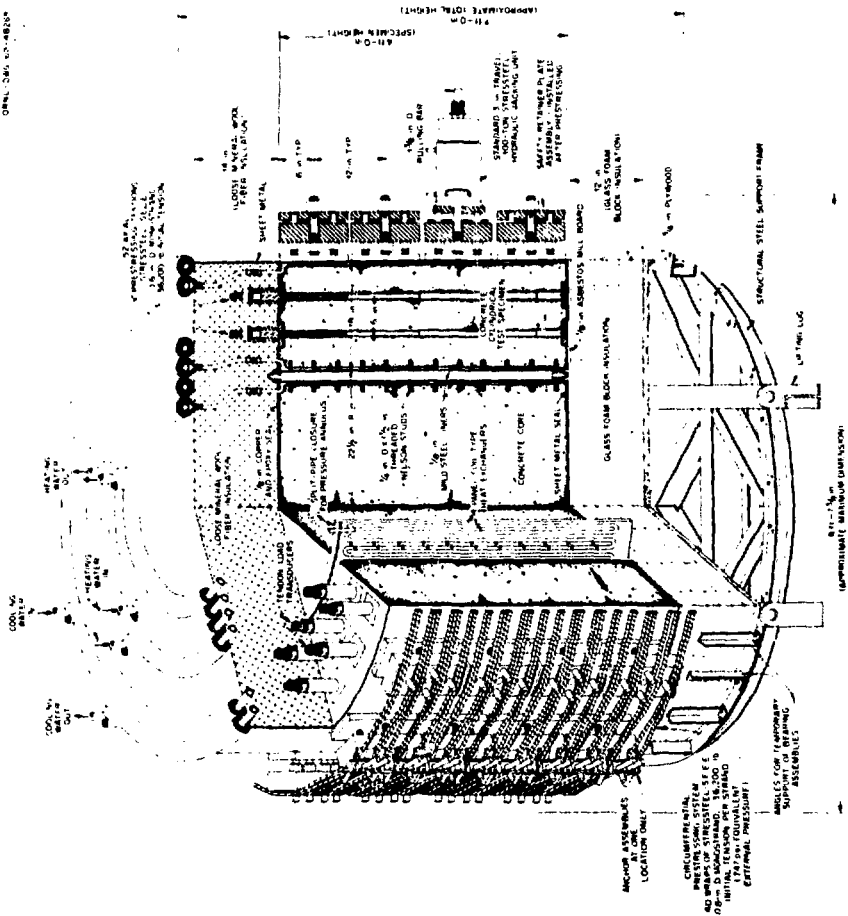
Fig. 7. Load vs time history of transducers on axial prestressing tendons CTR-1, CTR-3, and CTR-4. (1 lb = .454 kg)

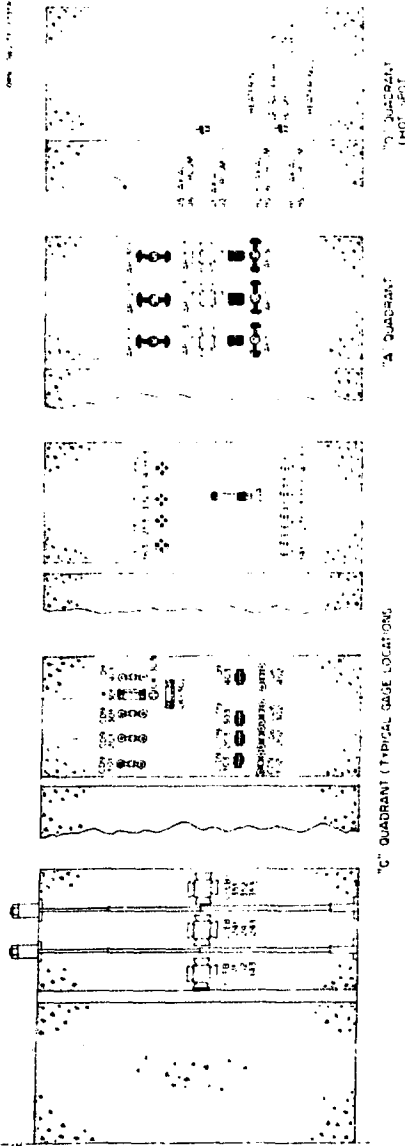


PRESTRESSED CONCRETE REACTOR VESSEL



THERMAL CYLINDER TEST SPECIMEN





Gage Designation

The first letter of the gage designation indicates in which of the four quadrant planes the gage is located (A, B, C or D). This is followed by one or two letters or a letter and number designating gage type. (See Table 1.) The first number of the three-number series which follows the letters indicates relative radial position progressing outwardly from the inside of the test section, and the last number indicates the orientation, i.e., 1 = axial, 2 = radial and 3 = circumferential. The middle number is used to further identify individual sensors. The gages adjacent to the hot spot were distinguished by the additional H3 letters.

ORNL-DWG 73-3720

